Available online at www.sciencedirect.com
ScienceDirect
Journal of Power Sources 172 (2007) 893–900
JOURNAL OF POWER SOURCES
www.elsevier.com/locate/jpowsour

# Cation ordering in the layered $Li_{1+x}(Ni_{0.425}Mn_{0.425}Co_{0.15})_{1-x}O_2$ materials ($x = 0$ and 0.12)

F. Weill [a,b], N. Tran [a], L. Croguennec [a,*], C. Delmas [a]

[a] *ICMCB, CNRS, Université Bordeaux 1 Site ENSCPB, 87 avenue Schweitzer, 33608 Pessac cedex, France*
[b] *Centre de Ressources en Microscopie Electronique et Microanalyse, Université Bordeaux I, 351 cours de la Libération, 33405 Talence, France*

Received 2 February 2007; received in revised form 19 April 2007; accepted 13 May 2007
Available online 26 May 2007

**Abstract**

The layered $Li_{1+x}(Ni_{0.425}Mn_{0.425}Co_{0.15})_{1-x}O_2$ ($x = 0$ and 0.12) materials were prepared by a coprecipitation method. Their structure was investigated using the combination of X-ray and electron diffraction experiments. For both materials ($x = 0$ and 0.12), the electron diffraction patterns revealed an in-plane $\sqrt{3}a_{hex.} \times \sqrt{3}a_{hex.}$ superstructure in agreement with the ordering of the $Li^+$, $Ni^{2+}$, $Ni^{3+}$, $Mn^{4+}$ and $Co^{3+}$ ions in the transition metal layers. The stoichiometry of these materials was not in agreement with an ideal ordering: the possible presence of point defects or of a domain microstructure was thus discussed. Electron diffraction also revealed that these ordered layers were slightly correlated along the $c_{hex.}$ axis for both materials.


*Keywords:* Layered oxides; Overlithiation; Cation mixing; X-ray diffraction; Electron diffraction; Lithium-ion battery

## 1. Introduction

In the framework of the development of new positive electrode materials for lithium-ion batteries to replace the widely used $LiCoO_2$ characterized by a too high cost for applications such as large batteries for electrical hybrid vehicles, many partial substitutions for Ni in $LiNiO_2$ were investigated [1–7]. Indeed, many drawbacks such as the difficulty to prepare a stoichiometric material [8–10], the poor capacity retention upon long range cycling [11] and the low thermal stability in the charged state [3,12,13] had to be overcome before the commercialization of the lithium nickelate derivatives as positive electrode material for lithium-ion batteries. Substituted $LiNiO_2$ (mainly cobalt and aluminium substituted) with optimized properties is now available and is used in a large number of applications [14]. More recently the Li(Ni, Mn)$O_2$ and Li(Ni, Mn, Co)$O_2$ systems were shown to be attractive due to promising electrochemical properties and to a good thermal stability in the charged state [6,15–19].

$LiNi_{1/2}Mn_{1/2}O_2$ can be considered as the end member of the solid solution $LiNi_{1/2-z/2}Mn_{1/2-z/2}Co_zO_2$ ($0 \le z \le 1$) and as a parent compound of $LiNi_{0.425}Mn_{0.425}Co_{0.15}O_2$ ($z = 0.15$). In $LiNi_{1/2}Mn_{1/2}O_2$, the nickel and manganese ions were shown by XPS and XANES data to be in the divalent and tetravalent oxidation states respectively [20,21]. Cation mixing was shown to occur between $Li^+$ ions from the interslab space and $Ni^{2+}$ ions from the slab, the amount of nickel ions present in the interslab space being in the range of 0.08–0.13 [16,22,23]. The presence of lithium ions in the (Ni, Mn) layers was evidenced by $^6$Li MAS NMR: in addition to a main signal at ~350 ppm corresponding to $Li^+$ ions in the interslab space, a small signal shifted to about 1500 ppm, similar to that observed for $Li_2MnO_3$ was assigned to a local environment $Li(OMn)_6$ in the slab [24,25]. Note that for $Li_{1-z}Ni_{1+z}O_2$ with a large departure from the stoichiometry, the presence of a large amount of $Ni^{2+}$ ions in the slabs leads also to a Li/Ni mixing between the slabs and the interslab spaces [26]. From a structural point of view, Meng et al. showed for $LiNi_{1/2}Mn_{1/2}O_2$ the presence of an in-plane $\sqrt{3}a_{hex.} \times \sqrt{3}a_{hex.}$ superstructure, which demonstrates that an ordering exists in

* Corresponding author. Tel.: +33 5 4000 2647/2234; fax: +33 5 4000 6698.
*E-mail address:* laurence.croguennec@icmcb-bordeaux.cnrs.fr (L. Croguennec).

0378-7753/$ – see front matter © 2007 Elsevier B.V. All rights reserved.
doi:10.1016/j.jpowsour.2007.05.090

the transition metal layers [27]. They proposed the $P\,3_112$ space group to describe the superstructure and a possible stacking of the ordered transition metal layers along the $c_{hex.}$ axis [27,28]. They also noted the material inhomogeneity at the crystal scale by the non observation of the superstructure in half of electron diffraction patterns.

In our lab, attention was paid to the $Li_{1+x}(Ni_{0.425}Mn_{0.425}Co_{0.15})_{1-x}O_2$ system [29]. From an electrochemical point of view, the reversible capacity in the 2–4.3 V range was shown to decrease with the increasing overlithiation ratio $x$, which was explained by a decreasing number of exchangeable electrons due to an increasing average transition metal oxidation state. In these $Li_{1+x}(Ni_{0.425}Mn_{0.425}Co_{0.15})_{1-x}O_2$ materials, the nickel, manganese and cobalt ions were shown, using X-ray photoelectron spectroscopy, to be as expected in the divalent/trivalent, tetravalent and trivalent state, respectively, overlithiation ($x>0$) leading to the presence of trivalent nickel ions for charge compensation [29].

As already reported in details in previous papers [29,30], the structure of $LiNi_{0.425}Mn_{0.425}Co_{0.15}O_2$ can be described in a hexagonal cell ($\alpha$-$NaFeO_2$ type structure; $R\bar{3}m$ space group) by the formula $(Li_{1-z}Ni_z)_{3b}(Li_zNi_{0.425-z}Mn_{0.425}Co_{0.15})_{3a}O_2$, that being in agreement with the experimental average oxidation state of 3.00 for the transition metal ions and with the chemical analyses. A cation mixing was thus shown to occur between $Li^+$ and $Ni^{2+}$ ions among the 3*a* and 3*b* sites and $z$ was found to be equal to 0.08. For the overlithiated $Li_{1.12}(Ni_{0.425}Mn_{0.425}Co_{0.15})_{0.88}O_2$ phase the crystallographic distribution can be described by the $(Li_{1-z}Ni_z)_{3b}(Li_{0.12+z}Ni_{0.374-z}Mn_{0.374}Co_{0.132})_{3a}O_2$ formula, in agreement with an experimental average oxidation state of 3.25 for the transition metal ions and with the chemical analyses [29]. $z$ was found to be equal to 0.02. Note that, in a first step, due to their very similar ionic radii, we assumed that the cation mixing occurs between $Li^+$ and $Ni^{2+}$ ions ($r(Ni^{2+})=0.69$ Å, $r(Li^+)=0.72$ Å, whereas $r(Mn^{4+})=0.54$ Å and $r(Co^{3+})=0.53$ Å). This hypothesis was supported by the combination of neutron diffraction data [31] and magnetic measurements [29]. Neutron diffraction experiments revealed that transition metal ions with a positive Fermi length must be present in the interslab space (*i.e.* Ni or Co ions). Furthermore, the magnetization versus field plots for slightly overlithiated phases showed at 5 K a significant remnant magnetization. Therefore these results confirm the presence of $Ni^{2+}$ ions in the lithium site, in agreement with previous studies [32]. The decreasing of the remnant magnetization with overlithiation was in good agreement with a decrease of the $Ni^{2+}$ ion amount in the interslab space and with the increase of the $Ni^{3+}$ ion amount in the slab. These structural models based on diffraction data (X-ray and neutron) and magnetic measurements were shown to describe rather well the average structure for these $Li_{1+x}(Ni_{0.425}Mn_{0.425}Co_{0.15})_{1-x}O_2$ phases ($x=0$ and 0.12) and have revealed a decrease in the amount of nickel ions in the interslab space and thus an increasing lamellar character of the structure with overlithiation. Nevertheless, they did not allow taking into account the appearance of small and broad peaks between 19.5° and 26° ($2\theta_{Cu}$). Fig. 1a shows a

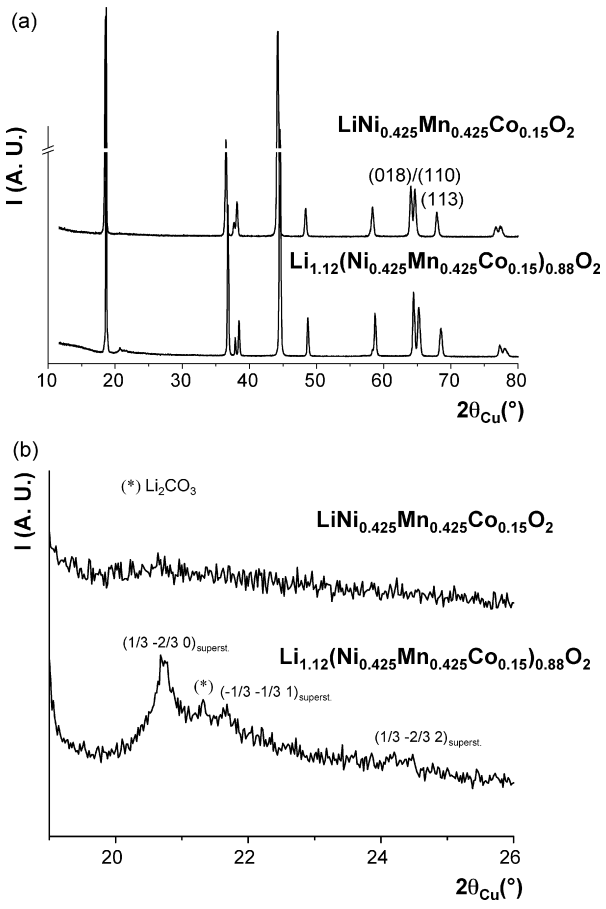


Fig. 1. (a) X-ray diffraction patterns of the $Li_{1+x}(Ni_{0.425}Mn_{0.425}Co_{0.15})_{1-x}O_2$ ($x=0$ and 0.12) materials (XRD recorded with a 40 s step duration); (b) detailed XRD data in the 19–26° ($2\theta_{Cu}$) range. The diffraction lines were indexed in the $R\bar{3}m$ space group with the $3a_{hex.} \times 3a_{hex.} \times c_{hex.}$ superstructure cell.

comparison of the X-ray diffraction patterns recorded for the $Li_{1+x}(Ni_{0.425}Mn_{0.425}Co_{0.15})_{1-x}O_2$ materials ($x=0$ and 0.12), with in Fig. 1b an enlargement in order to highlight the small lines mentioned just before. As suggested by Dahn and coworkers for the $Li[Ni_xLi_{(1/3-2x/3)}Mn_{(2/3-x/3)}]O_2$ materials [22] and as recently shown experimentally by Meng et al. using electron diffraction for those materials [27], the small lines observed between 19.5° and 26° ($2\theta_{Cu}$) are probably due to an ordering of the Li, Ni, Mn and Co ions in the transition metal layers, by analogy to the $Li_2MnO_3$ structure, thus leading to the occurrence of a superlattice.

In this study, we performed electron diffraction experiments to characterize the possible presence of an ordering in the structure of these $Li_{1+x}(Ni_{0.425}Mn_{0.425}Co_{0.15})_{1-x}O_2$ phases ($x=0$ and 0.12).

## 2. Experimental

$Ni(NO_3)_2{\cdot}6H_2O$ (97% Prolabo), $Mn(NO_3)_2{\cdot}4H_2O$ (98% Fluka), $Co(NO_3)_2{\cdot}6H_2O$ (98% Prolabo), LiOH (98+% Alfa Aesar) and $NH_4OH$ (28–30% J.T. Baker) were used as starting materials. The $Li_{1+x}(Ni_{0.425}Mn_{0.425}Co_{0.15})_{1-x}O_2$ ($x=0$ and 0.12) materials were prepared using the coprecipitation

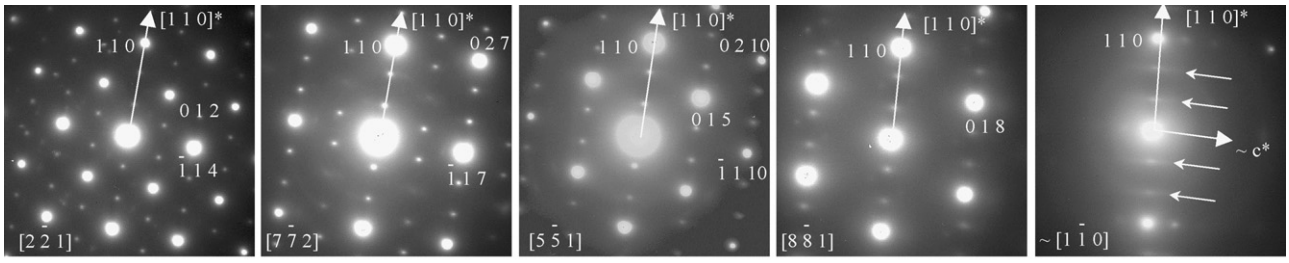


Fig. 2. Electron diffraction patterns of $Li_{1.12}(Ni_{0.425}Mn_{0.425}Co_{0.15})_{0.88}O_2$ indexed in the $a_{hex.} \times a_{hex.} \times c_{hex.}$ unit cell described in the $R\bar{3}m$ space group: (a) $[2\,\bar{2}\,1]_{hex.}$, (b) $[7\,\bar{7}\,2]_{hex.}$, (c) $[5\,\bar{5}\,1]_{hex.}$, (d) $[8\,\bar{8}\,1]_{hex.}$ and (e) $\sim[1\,\bar{1}\,0]_{hex.}$ zone axis patterns. The series is obtained by rotation around the [1 1 0]* axis (highlighted by the arrow). The angles between the consecutive patterns are, respectively: 15.8°, 9.5°, 10.1° and ~14.4°. Due to a tilt angle limited to 45°, the [1 $\bar{1}$ 0] zone axis pattern could not be reached.

method [33]. A mixed (1 M) aqueous solution of $Ni(NO_3)_2$, $Mn(NO_3)_2$ and $Co(NO_3)_2$ prepared with the 42.5/42.5/15 molar ratio was added drop wise through a burette into a basic solution (LiOH (1 M)/$NH_4OH$ (3 M)) under magnetic stirring. Note that the nominal Li/(Ni + Co + Mn) ratio was adjusted to 1.00 and 1.50 for $LiNi_{0.425}Mn_{0.425}Co_{0.15}O_2$ and $Li_{1.12}(Ni_{0.425}Mn_{0.425}Co_{0.15})_{0.88}O_2$, respectively. A green-brown mixed hydroxide was precipitated. Water was removed by evaporation at 80 °C under primary vacuum using a rotavapor device. The resulting wet precipitate was dried overnight at 105 °C, precalcined at 500 °C for 5 h in air and then calcined at 1000 °C for 12 h in air in a tubular furnace. Heating up speed was fixed to 5 °C $min^{-1}$ and cooling down speed was fixed to 4 °C $min^{-1}$.

The materials were analyzed by X-ray diffraction (XRD) using a Siemens D5000 diffractometer equipped with a diffracted-beam monochromator (Cu Kα radiation) in the 5–120° ($2\theta_{Cu}$) range in steps of 0.02° ($2\theta_{Cu}$) with a constant counting time of 40 s (or 108 s).

Li, Ni, Mn and Co contents in the materials were analyzed using inductively coupled plasma spectroscopy. The average oxidation state of the transition metal ions was determined by iodometric titration with $Na_2S_2O_3$. The average mass percentage of metal ions was checked by complexometric titration with EDTA. The materials synthesized with a nominal Li/(Ni + Co + Mn) ratio equal to 1.00 and 1.50, respectively, were shown to be indeed $LiNi_{0.425}Mn_{0.425}Co_{0.15}O_2$ ($x = 0$) and $Li_{1.12}(Ni_{0.425}Mn_{0.425}Co_{0.15})_{0.88}O_2$ ($x = 0.12$) phases, respectively.

For the electron diffraction experiments, a JEOL 2000FX microscope, equipped with a double tilt specimen stage, was used at an accelerating voltage of 200 kV. Previously to the observation, a suspension was obtained by grinding the materials in ethanol, a droplet of this suspension being deposited on a lacey carbon grid.

## 3. Results

### 3.1. $Li_{1.12}(Ni_{0.425}Mn_{0.425}Co_{0.15})_{0.88}O_2$

Fig. 2 shows a series of electron diffraction patterns collected from the same $Li_{1.12}(Ni_{0.425}Mn_{0.425}Co_{0.15})_{0.88}O_2$ crystal, these patterns were obtained by rotation around the [1 1 0]* axis. Note that these patterns were found to be representative of all the crystals in $Li_{1.12}(Ni_{0.425}Mn_{0.425}Co_{0.15})_{0.88}O_2$. The fundamental reflections can be indexed based on the parent hexagonal cell, in the $R\bar{3}m$ space group with the lattice parameters $a_{hex.} = 2.858$ Å and $c_{hex.} = 14.22$ Å. Additional weak superstructure reflections are observed, as shown for instance in the $[2\,\bar{2}\,1]_{hex.}$, $[7\,\bar{7}\,2]_{hex.}$ and $[5\,\bar{5}\,1]_{hex.}$ zone axis patterns. They are located along reciprocal directions running through the main reflections and parallel to the [1 1 0]* axis, dividing by three the distance between two successive main reflections along these directions. The presence of these superstructure reflections is consistent

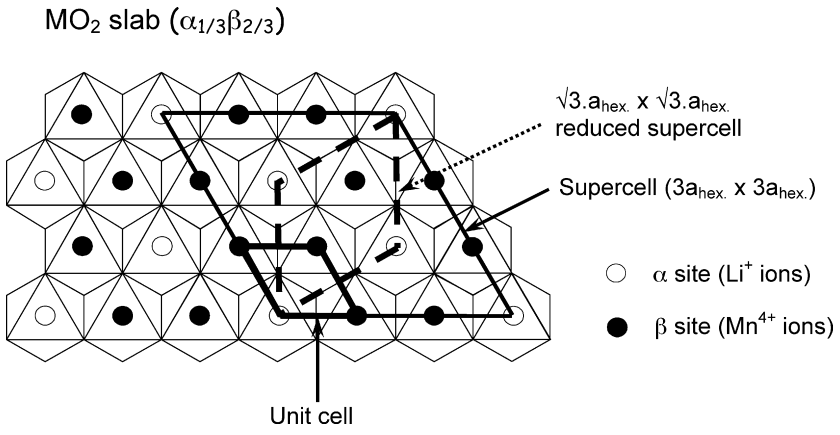


Fig. 3. Ideal cation ordering in the transition metal layers of $Li_2MnO_3$ ($Li(Li_{1/3}Mn_{2/3})O_2$).

with the formation of a $\sqrt{3}a_{hex.} \times \sqrt{3}a_{hex.}$ superstructure in the plane of the slabs. This superstructure, previously reported for $Li_2MnO_3$ [34] and $LiNi_{1/2}Mn_{1/2}O_2$ [27,35], implies as described in Fig. 3 in the case of $Li_2MnO_3$ the ordering of the Li, Ni, Mn and Co ions among two different sites (α and β) in the slabs. Due to the difference in size between these cations ($r(Ni^{2+}) = 0.69$ Å; $r(Li^+) = 0.72$ Å; $r(Co^{3+}) = 0.53$ Å; $r(Mn^{4+}) = 0.54$ Å; $r(Ni^{3+}) = 0.56$ Å) and to the stoichiometry, the large $Li^+$ and $Ni^{2+}$ ions are expected to occupy the α site while the small $Mn^{4+}$, $Ni^{3+}$ and $Co^{3+}$ ions should occupy the β site. Note that due to a ratio of 0.27/0.73 between the amounts of large and small cations present in the slabs, significantly different from that of 0.333/0.667 expected for an ideal $\sqrt{3}a_{hex.} \times \sqrt{3}a_{hex.}$ superstructure, the ordering can not be ideal.

The patterns given in Fig. 2 and obtained from the $[2\,\bar{2}\,1]_{hex.}$ zone axis pattern by rotation around the [1 1 0]* axis with high tilt angles show elongated superstructure reflections: the higher the angle is the more elongated are the reflections. Indeed, as shown by the last pattern obtained in Fig. 2e, close to the $[1\,\bar{1}\,0]_{hex.}$ zone axis pattern, streakings appear instead of superstructure reflections. Note that due to a tilt angle limited to 45° for the microscope, the $[1\,\bar{1}\,0]_{hex.}$ zone axis could not be reached exactly on this crystal. In order to confirm this behaviour another series of electron diffraction patterns was collected from another crystal of $Li_{1.12}(Ni_{0.425}Mn_{0.425}Co_{0.15})_{0.88}O_2$ and obtained also by tilting around the [1 1 0]* axis (Fig. 4). This series clearly demonstrates that, upon tilting around the [1 1 0]* axis, the extra spots observed in the $[8\,\bar{8}\,1]_{hex.}$ zone axis pattern (Fig. 4a) evolve to streakings in the $[1\,\bar{1}\,0]_{hex.}$ zone axis pattern (Fig. 4c). In order to highlight this evolution and the correlation between the extra spots and the streakings, the three dimensional reciprocal space was built in Fig. 5 from the diffraction patterns given in Fig. 2. The pattern corresponding to the $[1\,\bar{1}\,0]$ zone axis was first represented, $c^*$ being vertical and [1 1 0]* pointing toward us. In addition to the main reflections (represented by •), diffuse lines were reported as black lines at 1/3 and 2/3 of the distance between the origin and the node 110. The pattern corresponding to the $[8\,\bar{8}\,1]$ zone axis was then added. Between the $c^*$ direction and $[\bar{1}\,1\,16]^*$ (both directions making a right angle with [1 1 0]*) there is an angle of 19.75°. Once again the main nodes are reported, as well as the elongated extra weak reflections. All the observed diffraction patterns obtained from the $[1\,\bar{1}\,0]$ zone axis pattern by rotation around [1 1 0]* were finally reported to obtain Fig. 5. Obviously, in the ($a^*$, $b^*$) plane the $\sqrt{3}a_{hex.} \times \sqrt{3}a_{hex.}$ superstructure reflections (also experimentally observed in Fig. 6 for $Li_{1.12}(Ni_{0.425}Mn_{0.425}Co_{0.15})_{0.88}O_2$) result from the intersection of the plane with the diffuse lines. If there was a perfect ordering along the $c^*$ direction the intensity would be restricted to the intersection points (spherical volume around the nodes and no diffusion between the nodes). If there was no correlation at all along this direction the intensity would be homogeneously distributed along the diffusion lines (elongation of the spots during the rotation). Obviously the set of experimental patterns shows that our material presents an intermediate case which indicates a disordering along the $c$ direction with correlation between the ordered planes. Indeed, a careful observation of the diffuse scattering lines (Fig. 4c) indicated that they are rather inhomogeneous in intensity, which suggests a slight correlation between the ordered transition metal layers along the $c$-axis. Note that these electron diffraction analyses are in really good agreement with the observations done by X-ray diffraction. Indeed, as shown in Fig. 1b, all the superstructure lines are broad, especially those affected by the $l$ Miller index and thus by the $c$-axis.

### 3.2. $LiNi_{0.425}Mn_{0.425}Co_{0.15}O_2$

In order to emphasize the effect of overlithiation on the cationic ordering a series of electron diffraction patterns, collected on the same $LiNi_{0.425}Mn_{0.425}Co_{0.15}O_2$ crystal, are reported on Fig. 7. They are also obtained by tilting around the [1 1 0]* axis. As observed for $Li_{1.12}(Ni_{0.425}Mn_{0.425}Co_{0.15})_{0.88}O_2$, there are, on the one hand, intense spots that can be indexed in the $R\bar{3}m$ space group with the lattice parameters $a_{hex.} = 2.879$ Å and $c_{hex.} = 14.28$ Å using the usual hexagonal cell and, on the other hand, streakings or extra

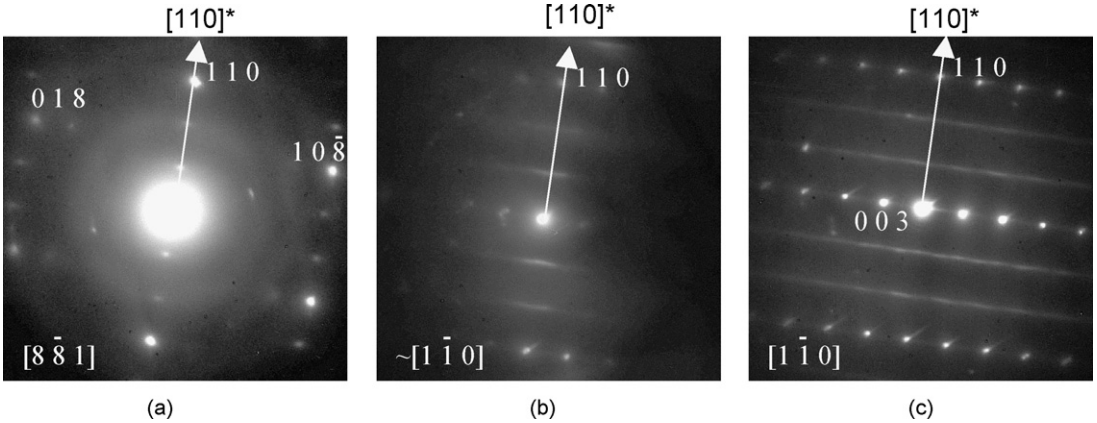


Fig. 4. Electron diffraction patterns of $Li_{1.12}(Ni_{0.425}Mn_{0.425}Co_{0.15})_{0.88}O_2$ indexed in the $a_{hex.} \times a_{hex.} \times c_{hex.}$ unit cell described in the $R\bar{3}m$ space group: (a) $[8\,\bar{8}\,1]_{hex.}$, (b) $\sim[1\,\bar{1}\,0]_{hex.}$ and (c) $[1\,\bar{1}\,0]_{hex.}$ zone axis patterns. The series is obtained by rotation around the [1 1 0]* axis (highlighted by the arrow). The angle between the patterns 4a and c is 19.75°.

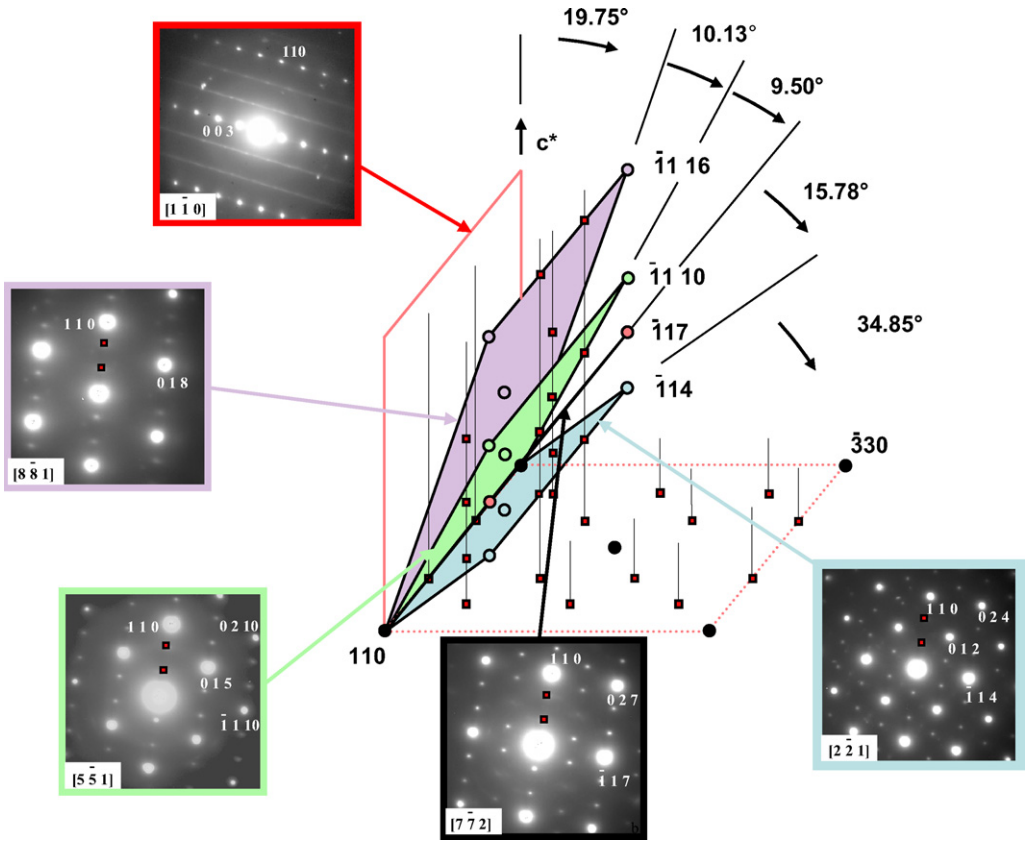


Fig. 5. Three-dimensional representation of the reciprocal space for the $Li_{1+x}(Ni_{0.425}Mn_{0.425}Co_{0.15})_{1-x}O_2$ materials; the electron diffraction patterns reported in Fig. 2 were indicated and distinguished by different colours. The main spots of the observed zone axis patterns are represented by (●) and the extra spots resulting from the superstructure by (■) The black lines link the extra spots along directions parallel to the $c^*$ axis and represent the disorder diffuse scattering lines.

spots, with a much weaker intensity, that can be explained by considering an in-plane $\sqrt{3}a_{hex.} \times \sqrt{3}a_{hex.}$ superstructure in the transition metal layers. From the $[7\,\bar{7}\,2]_{hex.}$ to the $[1\,\bar{1}\,0]_{hex.}$ zone axis patterns, well defined spots (Fig. 7a), then elongated spots (Fig. 7b), and finally streakings (Fig. 7d)

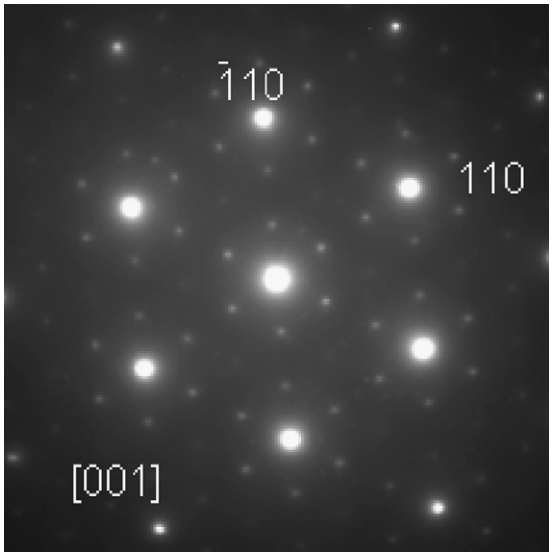


Fig. 6. [0 0 1] zone axis electron diffraction pattern of $Li_{1.12}(Ni_{0.425}Mn_{0.425}Co_{0.15})_{0.88}O_2$ materials.

were observed exactly at the same position as those recorded for $Li_{1.12}(Ni_{0.425}Mn_{0.425}Co_{0.15})_{0.88}O_2$. This evolution revealed also for $LiNi_{0.425}Mn_{0.425}Co_{0.15}O_2$ the existence of disorder diffuse scattering lines with an inhomogeneous intensity in the reciprocal space, which indicated that the ordered transition metal layers were only slightly correlated along the $c$-axis. Fig. 8 shows the comparison between the $[7\,\bar{7}\,2]_{hex.}$ zone axis patterns obtained for $Li_{1.12}(Ni_{0.425}Mn_{0.425}Co_{0.15})_{0.88}O_2$ (Fig. 2b) and $LiNi_{0.425}Mn_{0.425}Co_{0.15}O_2$ (Fig. 7a); a significant intensity difference for the superstructure spots (relatively to that of the main spots) was observed; this intensity was much lower for $LiNi_{0.425}Mn_{0.425}Co_{0.15}O_2$ despite a higher counting time for collecting the data, as clearly shown by the higher diameter of the central intense spot. This intensity difference observed in electron diffraction can be correlated to that observed in X-ray diffraction. Indeed, as shown in Fig. 1b, the superstructure reflections observed in the X-ray diffraction pattern of $LiNi_{0.425}Mn_{0.425}Co_{0.15}O_2$ were much weaker than those observed for $Li_{1.12}(Ni_{0.425}Mn_{0.425}Co_{0.15})_{0.88}O_2$. For the $LiNi_{0.425}Mn_{0.425}Co_{0.15}O_2$ phase, the material stoichiometry, with a ratio of 0.425/0.575 between the amounts of large ($Li^+$, $Ni^{2+}$) and small ($Mn^{4+}$, $Co^{3+}$) cations in the slab, is significantly different from that of 0.333/0.667 expected for a perfect $\sqrt{3}a_{hex.} \times \sqrt{3}a_{hex.}$ superstructure and from that of 0.27/0.73 obtained for $Li_{1.12}(Ni_{0.425}Mn_{0.425}Co_{0.15})_{0.88}O_2$.

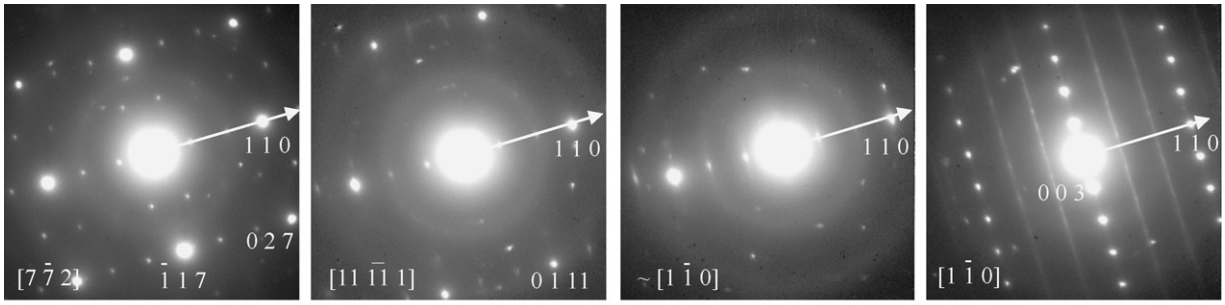


Fig. 7. Electron diffraction patterns of $LiNi_{0.425}Mn_{0.425}Co_{0.15}O_2$ indexed in the $a_{hex.} \times a_{hex.} \times c_{hex.}$ unit cell described in the $R\bar{3}m$ space group: (a) $[7\,\bar{7}\,2]_{hex.}$, (b) $[11\,\bar{1}\,\bar{1}\,1]_{hex.}$, (c) $\sim[1\,\bar{1}\,0]_{hex.}$ and (d) $[1\,\bar{1}\,0]_{hex.}$ zone axis patterns. The series is obtained by rotation around the [1 1 0]* axis. The angles between the patterns 7a and c is 14.63° and between 7c and d is 24.73°.

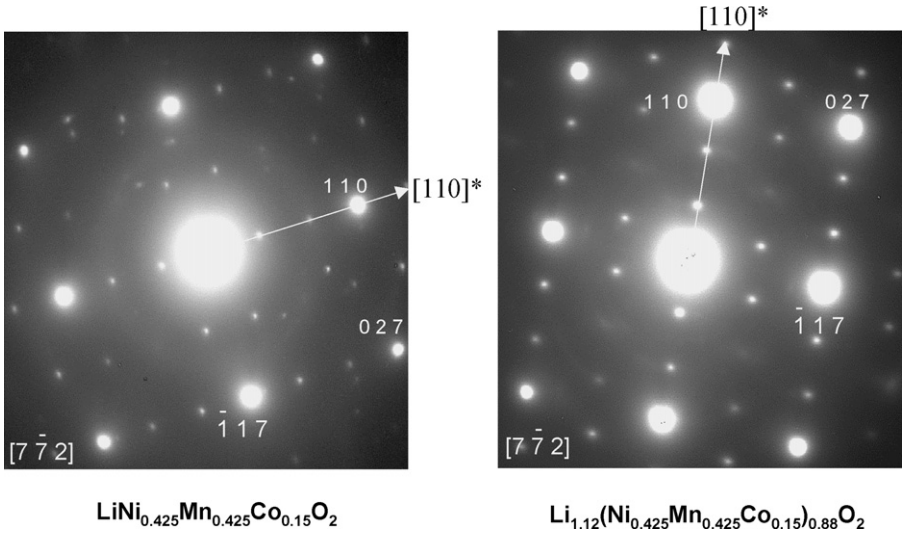


Fig. 8. Electron diffraction $[7\,\bar{7}\,2]_{hex.}$ zone axis patterns obtained for $LiNi_{0.425}Mn_{0.425}Co_{0.15}O_2$ and $Li_{1.12}(Ni_{0.425}Mn_{0.425}Co_{0.15})_{0.88}O_2$.

## 4. Discussion

As shown by the electron diffraction patterns recorded for the $Li_{1+x}(Ni_{0.425}Mn_{0.425}Co_{0.15})_{1-x}O_2$ ($x = 0$ and 0.12) materials and as discussed schematically in Fig. 5, a similar in-plane $\sqrt{3}a_{hex.} \times \sqrt{3}a_{hex.}$ superstructure exists in the slab between the Li and transition metal ions for both compositions. By analogy with $Li_2MnO_3$ one can assume that the Li, Ni, Mn and Co ions would be distributed among two sites (α and β) in the slab; in respect with their relative ionic radii and with the stoichiometry of these materials, the $Ni^{2+}$ and $Li^+$ ions would preferentially occupy the α site whereas the $Ni^{3+}$, $Co^{3+}$ and $Mn^{4+}$ would occupy the β site. Such an ordering would lead to a minimization of the strains in the slabs and thus to a stabilization of these structures with four or five cations ($Li^+$, $Ni^{2+}/Ni^{3+}$, $Mn^{4+}$ and $Co^{3+}$ ions) in the same environment. According to the cationic distributions determined for $LiNi_{0.425}Mn_{0.425}Co_{0.15}O_2$ and $Li_{1.12}(Ni_{0.425}Mn_{0.425}Co_{0.15})_{0.88}O_2$ from the refinement of their X-ray and neutron diffraction data, the distributions of the various cations in the α and β sites were calculated and summarized in Table 1. For $LiNi_{0.425}Mn_{0.425}Co_{0.15}O_2$, as the amount of large cations ($Li^+ + Ni^{2+}$) in the slab was larger than 0.333, the preferential presence of $Li^+$ ions in the α site was assumed, leading to the presence of 0.09 $Ni^{2+}$ ions in the β site. In the same way, for $Li_{1.12}(Ni_{0.425}Mn_{0.425}Co_{0.15})_{0.88}O_2$, the amount of small cations ($Mn^{4+}$, $Ni^{3+}$ and $Co^{3+}$) is larger than 0.667, leading to the presence of 0.08 small cations in the α site (as reported in Table 1, we arbitrarily assumed they were $Ni^{3+}$ ions because these ions are slightly larger than $Co^{3+}$ and $Mn^{4+}$). The amount of defects, *i.e.* the presence of large cations in theoret-

Table 1
Cationic distributions in the α and β sites for the $Li_{1+x}(Ni_{0.425}Mn_{0.425}Co_{0.15})_{1-x}O_2$ ($x = 0$ and 0.12) materials

| Nominal formula | $LiNi_{0.425}Mn_{0.425}Co_{0.15}O_2$ | $Li_{1.12}(Ni_{0.425}Mn_{0.425}Co_{0.15})_{0.88}O_2$ | $Li_2MnO_3$ [34] |
|---|---|---|---|
| Slab cationic distribution | $[Li^+_{0.07}Ni^{2+}_{0.355}Mn^{4+}_{0.425}Co^{3+}_{0.15}]$ | $[Li^+_{0.14}Ni^{2+}_{0.114}Ni^{3+}_{0.24}Mn^{4+}_{0.374}Co^{3+}_{0.132}]$ | $[Li^+_{0.33}Mn^{4+}_{0.67}]$ |
| Cationic distributions in the α and β sites | α ($Li^+_{0.07}Ni^{2+}_{0.263}$) β ($\underline{Ni^{2+}}_{0.092}$, $Mn^{4+}_{0.425}Co^{3+}_{0.15}$) | α ($Li^+_{0.14}Ni^{2+}_{0.114}\underline{Ni^{3+}}_{0.079}$) β ($Ni^{3+}_{0.161}Mn^{4+}_{0.374}Co^{3+}_{0.132}$) | α ($Li^+_{0.33}$) β ($Mn^{4+}_{0.66}$) |

The data were compared to those of $Li_2MnO_3$. The cations "unexpected" in the α and β sites were underlined.

ically small β sites or of small cations in theoretically large α sites, was larger for $Li_{1.12}(Ni_{0.425}Mn_{0.425}Co_{0.15})_{0.88}O_2$ (~25% versus ~14% for $LiNi_{0.425}Mn_{0.425}Co_{0.15}O_2$), suggesting higher constraints in the slabs for the latter.

As mentioned previously, a better contrast is observed in X-ray diffraction (resp. in electron diffraction) between the α and β sites with increasing overlithiation, leading to a better resolution of the superlattice reflections (resp. intensity of the superlattice spots vs. that of the fundamental reflections) for $Li_{1.12}(Ni_{0.425}Mn_{0.425}Co_{0.15})_{0.88}O_2$: indeed, assuming the cation orderings reported in Table 1, the $f_\alpha/f_\beta$ ratio between the X-ray scattering factors associated to the two α and β sites evolves from 0.93 for $LiNi_{0.425}Mn_{0.425}Co_{0.15}O_2$ to 0.69 for $Li_{1.12}(Ni_{0.425}Mn_{0.425}Co_{0.15})_{0.88}O_2$ and becomes thus significantly different from 1 with increasing overlithiation. Note that for $Li_2MnO_3$, this $f_\alpha/f_\beta$ ratio is equal to 0.1, leading thus to an even better observation of the superlattice reflections [35].

As the ratio between the large and small cations is not in agreement with a (0.333/0.667) distribution, the cation ordering observed in the slab for these materials could be associated either to the existence of some perfectly $\sqrt{3}a_{hex.} \times \sqrt{3}a_{hex.}$ ordered domains separated by non ordered domains, those latter being different in composition and rich in large or in small cations in order to accommodate the overall average composition, or to the presence of randomly distributed defects in a perfectly ordered slab. Note that for the $Li[Ni_xLi_{(1/3-2x/3)}Mn_{(2/3-x/3)}]O_2$ materials, the presence of ordered microdomains in the slabs was suggested by HRTEM and $^6Li$ NMR [36,37]. On the basis of our electron diffraction results only, it was not possible to clearly define the nature of the defects in the slabs; microdiffraction patterns combined with EDX and EELS spectroscopic analyses would be necessary to confirm one or the other hypothesis. Nevertheless, because all the superlattice lines observed for $Li_{1.12}(Ni_{0.425}Mn_{0.425}Co_{0.15})_{0.88}O_2$ are broad, as shown in Fig. 1b, and especially those with Miller index $l \neq 0$, it can be noted that there are at least two possible origins for this broadening:

(i) If point defects only existed in the slabs, then this broadening of the superlattice lines would be only explained by the quasi-absence of correlation between the ordered slabs along the $c_{hex.}$ axis. Note that, depending on the synthesis conditions, $Li_2MnO_3$ can be characterized by ordered slabs more or less correlated along the $c_{hex.}$ axis, despite the accurate stoichiometry for a $\sqrt{3}a_{hex.} \times \sqrt{3}a_{hex.}$ superstructure: indeed, at low synthesis temperature ($T < 900\,^\circ C$), the superlattice lines are also very broad [38].

(ii) If the slabs were characterized by ordered domains separated by non ordered domains, with local composition variations and strains, it would also lead to a broadening of all the superlattice lines. Furthermore, a domain microstructure in the slabs would also lead directly to a lack of correlation along the $c_{hex.}$ axis and thus to an even larger broadening of the superstructure lines. From a general point of view, the ordering is often observed by diffraction techniques far from ideal compositions, consequently in our case there is no experimental reason to favour the existence of well-ordered micro-domains which would induce strong local changes in compositions.

## 5. Conclusions

In this work, we have studied the $LiNi_{0.425}Mn_{0.425}Co_{0.15}O_2$ and $Li_{1.12}(Ni_{0.425}Mn_{0.425}Co_{0.15})_{0.88}O_2$ materials from a structural point of view by combining X-ray and electron diffraction data. For both $LiNi_{0.425}Mn_{0.425}Co_{0.15}O_2$ and $Li_{1.12}(Ni_{0.425}Mn_{0.425}Co_{0.15})_{0.88}O_2$ materials, electron diffraction patterns showed the presence of an ordering in the transition metal layers, *i.e.* an in-plane $\sqrt{3}a_{hex.} \times \sqrt{3}a_{hex.}$ superstructure with two different sites (α and β) that are expected to be occupied preferentially by ($Li^+$, $Ni^{2+}$) ions and ($Ni^{3+}$, $Mn^{4+}$, $Co^{3+}$) ions, respectively, due to the difference in their ionic radii. This study suggests that this cation ordering allows stabilizing these structures and is always observed whatever the composition. However, for the $Li_{1+x}(Ni_{0.425}Mn_{0.425}Co_{0.15})_{1-x}O_2$ materials ($x = 0$ and 0.12) as the ratio between large and small cations is far from the ideal one of (1:2), point defects or a domain microstructure are thus expected. Electron diffraction data clearly showed diffuse disorder scattering lines, with an inhomogeneous intensity and parallel to the $c_{hex.}^*$ axis, which was attributed to a slight correlation between the ordered transition metal layers along the $c_{hex.}$ axis. This absence of any long range ordering along the $c_{hex.}$ axis explains why it is not possible to fit the experimental XRD pattern of $Li_{1.12}(Ni_{0.425}Mn_{0.425}Co_{0.15})_{0.88}O_2$ using any 3D space group to describe the superlattice. Indeed, the refinement always leads to unsatisfactory results concerning the superstructure lines. This absence of any long range ordering along the $c_{hex.}$ axis was expected if one considers that the driving force for ordering is generally the difference in ionic radius and not the difference in charge. Within the slabs the difference in size is high enough to induce an ordering, on the contrary the local differences in slab thickness are averaged by the oxygen layers and therefore prevent any noticeable ordering along the c-axis.

## Acknowledgements

The authors are grateful to C. Denage (ICMCB, Pessac, France) for technical assistance, to C. Jordy, Ph. Biensan (SAFT, Bordeaux, France) and Y. Shao-Horn (MIT, Cambridge, USA) for fruitful discussions, and to SAFT and Région Aquitaine for financial support.

## References

[1] C. Delmas, I. Saadoune, Solid State Ionics 53-56 (1992) 370.
[2] C. Delmas, I. Saadoune, A. Rougier, J. Power Sources 43-44 (1993) 595.
[3] T. Ohzuku, A. Ueda, M. Kouguchi, J. Electrochem. Soc. 142 (1995) 4033.
[4] Q. Zhong, U. Von Sacken, J. Power Sources 54 (1995) 221.
[5] C. Pouillerie, F. Perton, P. Biensan, J.-P. Pérès, M. Broussely, C. Delmas, J. Power Sources 96 (2001) 293.
[6] Y. Makimura, T. Ohzuku, J. Power Sources 119 (2003) 156.
[7] L. Croguennec, E. Suard, P. Willmann, C. Delmas, Chem. Mater. 14 (2002) 2149.

[8] P.G. Bruce, A. Lisowska-Oleksiak, M.Y. Saidi, C.A. Vincent, Solid State Ionics 57 (1992) 353.
[9] R. Kanno, H. Kubo, Y. Kawamoto, T. Kamiyama, F. Izumi, Y. Takeda, M. Takano, J. Solid State Chem. 110 (1994) 216.
[10] J.P. Pérès, C. Delmas, A. Rougier, M. Broussely, F. Perton, P. Biensan, P. Willmann, J. Phys. Chem. Solids 57 (1996) 1057.
[11] M. Broussely, F. Perton, P. Biensan, J.M. Bodet, J. Labat, A. Lecerf, C. Delmas, A. Rougier, J.P. Pérès, J. Power Sources 54 (1995) 109.
[12] J.R. Dahn, E.W. Fuller, M. Obrovac, U. Von Sacken, Solid State Ionics 69 (1994) 265.
[13] H. Arai, S. Okada, Y. Sakurai, J. Yamaki, Solid State Ionics 109 (1998) 295.
[14] A. Broussely, P. Blanchard, P. Biensan, J.P. Planchat, K. Nechev, R.J. Staniewicz, J. Power Sources 119 (2003) 859.
[15] T. Ohzuku, Y. Makimura, Chem. Lett. (2001) 642.
[16] T. Ohzuku, Y. Makimura, Chem. Lett. (2001) 744.
[17] S.W. Oh, S.H. Park, C.W. Park, Y.K. Sun, Solid State Ionics 171 (2004) 167.
[18] S. Jouanneau, J.R. Dahn, J. Electrochem. Soc. 151 (2004) A1749.
[19] S. Jouanneau, D.D. MacNeil, Z. Lu, S.D. Beattie, G. Murphy, J.R. Dahn, J. Electrochem. Soc. 150 (2003) A1299.
[20] K.M. Shaju, G.V.S. Rao, B.V.R. Chowdari, Electrochim. Acta 48 (2003) 1505.
[21] W.S. Yoon, C.P. Grey, M. Balasubramanian, X.Q. Yang, J. McBreen, Chem. Mater. 15 (2003) 3161.
[22] Z.H. Lu, L.Y. Beaulieu, R.A. Donaberger, C.L. Thomas, J.R. Dahn, J. Electrochem. Soc. 149 (2002) A778.
[23] Z.H. Lu, Z.H. Chen, J.R. Dahn, Chem. Mater. 15 (2003) 3214.
[24] W. Yoon, Y. Paik, X. Yang, M. Balasubramanian, J. McBreen, C. Grey, Electrochem. Solid State Lett. 5 (2002) A263.
[25] X.Q. Yang, J. McBreen, W.S. Yoon, C.P. Grey, Electrochem. Comm. 4 (2002) 649.
[26] C. Pouillerie, E. Suard, C. Delmas, J. Solid State Chem. 158 (2001) 187–197.
[27] Y.S. Meng, G. Ceder, C.P. Grey, W.S. Yoon, Y. Shao Horn, Electrochem. Solid State Lett. 7 (2004) A155.
[28] Y. Koyama, N. Yabuuchi, I. Tanaka, H. Adachi, T. Ohzuku, J. Electrochem. Soc. 151 (2004) A1545.
[29] N. Tran, L. Croguennec, C. Labrugère, C. Jordy, P. Biensan, C. Delmas, J. Electrochem. Soc. 153 (2006) A261–A269.
[30] N. Tran, L. Croguennec, C. Jordy, P. Biensan, C. Delmas, Solid State Ionics 176 (2005) 1539.
[31] N. Tran, Ph.D. Thesis, University Bordeaux I, 2005.
[32] A.L. Barra, G. Chouteau, A. Stepanov, A. Rougier, C. Delmas, Eur. Phys. J. B 7 (1999) 551.
[33] D. Caurant, N. Baffier, B. Garcia, J.P. Pereira-Ramos, Solid State Ionics 91 (1996) 45.
[34] P. Strobel, B. Lambertandron, J. Solid. State Chem. 75 (1988) 90.
[35] Y.S. Meng, G. Ceder, C.P. Grey, W.S. Yoon, M. Jiang, J. Bréger, Y. Shao Horn, Chem. Mater. 17 (2005) 2386.
[36] J.S. Kim, C.S. Johnson, J.T. Vaughey, M.M. Thackeray, S.A. Hackney, Chem. Mater. 16 (2004) 1996.
[37] W.S. Yoon, C.P. Grey, M. Balasubramanian, X.Q. Yang, D.A. Fischer, J. McBreen, Electrochem. Solid State Lett. 7 (2004) A53.
[38] Y.S. Hong, Y.J. Park, K.S. Ryu, S.H. Chang, Solid State Ionics 176 (2005) 1035.